Genomes & Developmental Control

Interactions between *HOXD* and *Gli3* genes control the limb apical ectodermal ridge via *Fgf10*

Jozsef Zakany, Giovanna Zacchetti, Denis Duboule *

*Department of Zoology and Animal Biology and National Research Centre 'Frontiers in Genetics', University of Geneva, Sciences III,
Quai Ernest Ansermet 30, 1211 Geneva 4, Switzerland*

Abstract

The development of the vertebrate limb is dependent upon two signaling centers, the apical ectodermal ridge (AER), which provides the underlying mesenchyme with essential growth factors, and the zone of polarizing activity (ZPA), the source of the *Sonic hedgehog* (SHH) product. Recent work involving gain and loss of function of *Hox* genes has emphasized their impact both on AER maintenance and *Shh* transcriptional activation. Here, we describe antagonistic interactions between posterior *Hoxd* genes and *Gli3*, suggesting that the latter product protects the AER from the deleterious effect of the formers, and we present evidence that *Fgf10* is the mediator of HOX-dependent AER expansion. Furthermore, the striking similarity between some of the hereby observed *Hox/Gli3*-dependent morphogenetic defects and those displayed by fetuses with severely altered retinoic acid metabolism suggests a tight connection between these various pathways. The nature of these potential interactions is discussed in the context of proximal–distal growth and patterning.
© 2007 Elsevier Inc. All rights reserved.

Keywords: Hox; Gli3; Fgf10; Limb development; Posterior prevalence; Collinearity; Mouse

Introduction

Genetic studies in mice have shown that limb growth and patterning critically depends upon *Hox* genes belonging to paralogy groups 9 to 13 of both the *HoxA* and *HoxD* clusters. Despite structural homology and genomic neighborhood, individual representatives of the different groups have distinct roles in the formation of particular limb regions. For example, in the absence of both *Hoxa13* and *Hoxd13* function, autopods (hands and feet) mostly fail to develop (Fromental-Ramain et al., 1996b; Kondo et al., 1997). Similarly, severe truncations of the zeugopod (forearm, or lower arm) were seen when removing group 11 function (Davis et al., 1995) and, likewise, group 9 deficit mostly affected the stylopod (humerus) (Fromental-Ramain et al., 1996a; Wellik and Capecchi, 2003). These analyses uncovered anatomical defects generally corresponding

in space and time to the expression domains of the genes concerned. In developing limbs, both the timing of expression and the position of the functional domains of the various *Hox* genes reflect their linear order along the chromosome (Kmita and Duboule, 2003). However, at the most proximal end of the stylopod *Hox* gene function seems to be somewhat dispensable (Kmita et al., 2005).

The importance and necessity for such a strict temporal-spatial distribution of gene expression domains along the proximo-distal limb axis has been illustrated by several approaches. Extensive rearrangements in the *HoxD* cluster induced limb anatomical defects due to the abnormal expression of *Hox* genes, rather than to their loss of function. When group 13 products were ectopically expressed in growing zeugopods, these segments were strongly affected, reminiscent of group 11 functional deficits. Related examples of forced expression of group 13 or 12 products in developing chick or mouse limbs resulted in similar patterning defects (Goff and Tabin, 1997; Williams et al., 2006). These observations gave support to the existence of functional interactions between *Hox* gene products, following the rule of

---

* Corresponding author. Present address: School of life Sciences, Ecole Polytechnique Federale Lausanne (EPFL), Switzerland. Fax: +41 22 3796795.
E-mail address: Denis.Duboule@zoo.unige.ch (D. Duboule).

posterior prevalence (Duboule, 1991; Duboule and Morata, 1994), whereby a 'posterior' or 'distal' gene product (e.g. HOXD13) can abrogate the function of a more 'anterior' or 'proximal' gene (e.g. group 11), likely at the post-transcriptional level (Herault et al., 1997; Spitz et al., 2003; van der Hoeven et al., 1996). During limb development, posterior prevalence has been documented at rather late stages, i.e. at times and in domains corresponding to distal pieces of the appendages, and the functional relevance of excluding distal *Hox* gene products from the early limb bud, such as to prevent distal structures to form at proximal locations, has not been assessed.

At the molecular level, posterior prevalence may result from interactions between HOX proteins either with various HOX partners, or with other gene products, leading for instance to the modulation of their functional activities and concurrent impact upon the regulation of target genes (Williams et al., 2006; Zappavigna et al., 1994). Among the few confirmed protein partners of HOX products (Capellini et al., 2006; Chen et al., 2004), the zinc finger domain transcription factor *Gli3* is of particular interest in this context. The *Gli3* gene product is critical for proper limb development, mainly through its antagonistic genetic interaction with *Shh*, as the stimulation of *Shh* signaling prevents the default processing of GLI3 from an activator to a repressor form (Litingtung et al., 2002; te Welscher et al., 2002; Wang et al., 2000), thereby up-regulating *Shh* target genes. In addition to this involvement in *Shh* signaling, *Gli3* and *Hoxd* genes were reported to interact during early limb development, in two different contexts. First, genetic evidence suggested that GLI3 acts as a negative regulator of several *Hoxd* genes, such as *Hoxd13* and *Hoxd12* during early limb budding (Buscher et al., 1997; Zuniga and Zeller, 1999). Secondly, GLI3 was shown to physically interact with the HOXD12 protein during distal limb patterning. In this latter case, the GLI3/HOXD12 interaction modified digit patterning, likely as a consequence of direct protein/protein contacts (Chen et al., 2004).

Mice carrying the *Extra-toes* (*Xt*) mutation lack the function of *Gli3*. These mice have a range of anomalies, among which a severe polydactyly of both fore-and hindlimbs, likely due to the de-repression of *Hox* genes, and concurrent ectopic expression of *Shh*, at the anterior margin of the developing limb (Buscher et al., 1997). In order to assess whether the wild-type pentadactyly was indeed due to a *Gli3*-dependent anterior repression of *Hox* genes, in other words whether the polydactyly observed in *Xt* mutant mice is dependent upon the gain of *Hox* gene function(s), we crossed *Xt* mice with mice carrying either a full, or a partial, deletion of the *HoxD* cluster (Zakany et al., 2001, 2004). Here, we show that removing all *Hoxd* gene function, in addition to *Gli3* in the developing autopod, does not significantly reduce the number of digits when compared to mice mutant for *Gli3* alone.

In striking contrast, however, the combination of the *Gli3* mutant allele with a partial deletion of the *HoxD* cluster (deletion of *Hoxd1* to *Hoxd10* included) gave mice with heavily truncated limbs, a situation drastically different from the phenotype observed with the same deletion, but in the presence of *Gli3* function. In this latter case, gain of function of the remaining 'posterior' *Hoxd* genes lead to an ectopic *Shh*

domain anteriorly and consequent bilateral symmetry of an otherwise weakly truncated limb (Zakany et al., 2004). This observation indicates that widespread and early expression of *Hoxd13* and *Hoxd12* can severely impair stylopod development, but only when *Gli3* function is either reduced or removed, suggesting that *Gli3* function protects against the prevalent function of posterior genes over their more anterior neighbors. Such severe limb truncations involved defects in the apical ectodermal ridge (AER), likely due to a dramatic decrease of *Fgf10* expression in limb bud mesenchyme. We discuss the potential roles of these various players in the growth and patterning of the limbs.

Materials and methods

Mouse stocks, crosses and genotyping of mid-gestation embryos and near-term fetuses

The mouse lines carrying the *HoxD* cluster alleles used in this study were produced by *loxP/Cre*-mediated site-specific recombination. *del(1–13)* is an approximately 100-kb large deletion encompassing from the *Hoxd1* to the *Hoxd13* loci. In this deletion, the entire *HoxD* function is lost (Zakany et al., 2001). *Del(1–10)* was generated by targeted meiotic recombination (Herault et al., 1998) using *del(1–13)* as one of the parental alleles to produce an approximately 70-kb large targeted deletion from *Hoxd1* to *Hoxd10* included (Zakany et al., 2004). The two deficiencies have the same breakpoint near *Hoxd1*. All *HoxD* alleles were genotyped in a multiplex PCR reaction, using the 5′-CCACCCTGCTAAATAAACGCTG-3′ *Hoxd11* forward primer, and the 5′-GGTTGCCTCTTTTCCTCTGTCTC-3′ *Hoxd10* reverse primer for wild-type and the 5′-CTATTCAAAGGTGGGGAGCAGTC-3′ *Hoxd1* reverse primer for mutant allele. *Gli3 XtJax* allele was genotyped with the 5′-TACC-CCAGCAGGAGACTCAGATTAG-3′ forward and 5′AAACCCGTGGCTCA-GAGCAAG-3′ reverse primers, while the *Gli3* wild-type allele with the 5′-GGGTGAACAGCATCAAAATGGAG-3′ forward and 5′-ATAGC-CATGTGGTGGTGCCCATG-3′ reverse primers.

Heterozygous males or females of either *HoxD* deficiencies were crossed over *Xt* heterozygous males or females to obtain compound heterozygous *Xt/+; del(1–13)/+* and *Xt/+;Del(1–10)/+* males and females. Both compound mutants were obtained in near Mendelian proportions, and most individuals of both genotypes displayed characteristic digit defects in forelimbs: olygodactyly in *Xt/+;del(1–13)/+*(Fig. 1E) and polydactyly in *Xt/+;Del(1–10)/+* (Fig. 1F). As *del(1–13)* homozygous animals are semi-lethal post-natally and both *Del(1–10)* and *Xt* homozygous animals are lethal at birth, we collected the F2 progeny from *Xt/+;del(1–13)/+* and *Xt/+;Del(1–10)/+* parents on the 18th day post-fertilization (E18) in order to minimize losses of individuals with compound genotypes. Genomic DNA was extracted from tail biopsies or yolk sac (E10, see below) and genotyped by PCR reactions, using the specific primers indicated above.

RNA in situ hybridization

To evaluate early limb development in the various genotypic classes, F2 embryos were collected on the morning of the 10th day of development (E10) and processed for whole mount RNA in situ hybridization following standard procedures (see e.g. www.eumorphia.org/EMPReSS/servlet/EMPReSS Doc. Number: 13_003). Yolk sac samples were collected individually and genomic DNA was isolated for genotyping, whereas individually fixed embryos were stored at minus 20 °C in methanol. Once genotypes were established, representatives of the selected genotypes were grouped and processed together for any given probe. Forelimb buds of all specimens were photographed and the same magnifications are shown. Probes were as originally described: *Fgf8* (Crossley and Martin, 1995), *Fgf10* (Bellusci et al., 1997), *Gli3* (Hui and Joyner, 1993), *Hoxd13* (Dolle et al., 1993), *Meis1* (Saleh et al., 2000) and *Shh* (Echelard et al., 1993). After the in situ hybridization patterns were documented, the embryos were homogenized, genomic DNA was extracted and the genotypes were further verified.
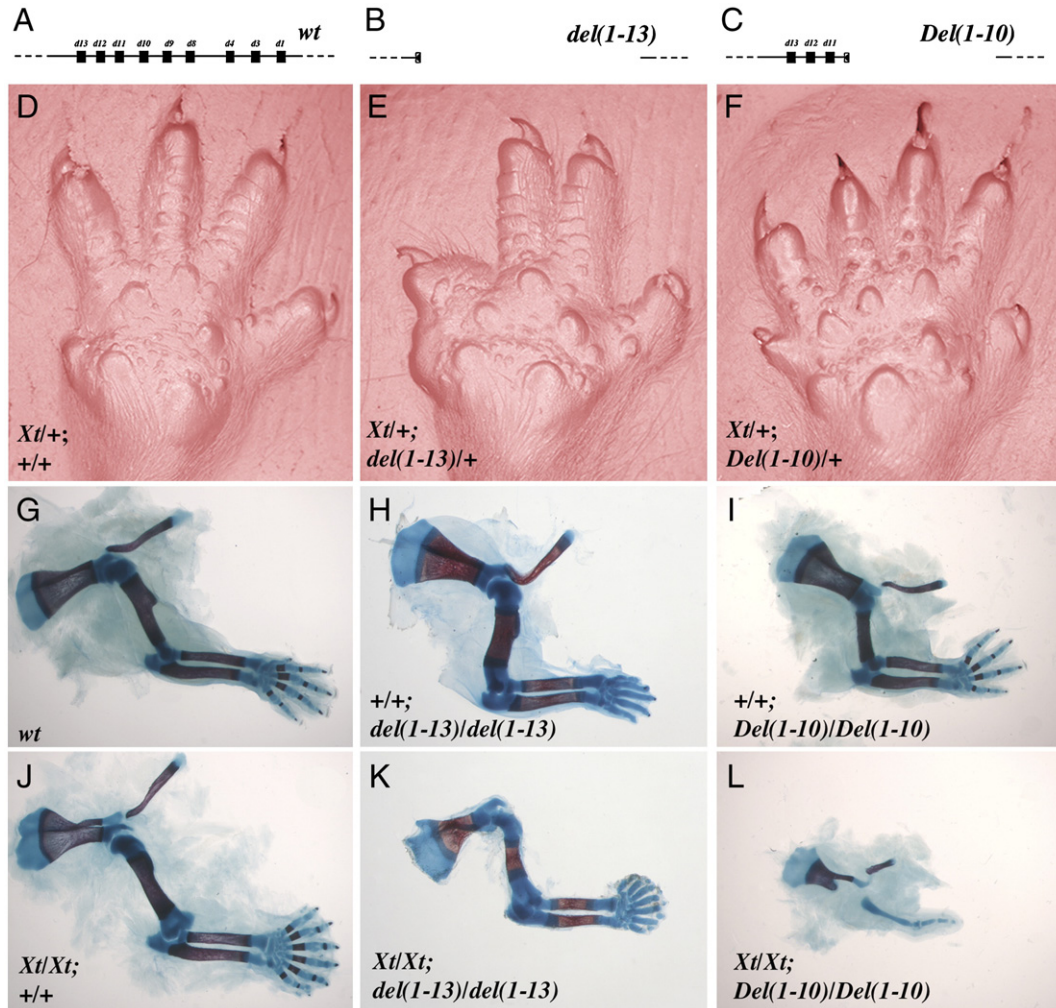
Fig. 1. Forelimb phenotypes of mice carrying either of two mutant alleles of the *HoxD* cluster *del(1–13)* or *Del(1–10)*, and the *Xt* allele at the *Gli3* locus. (A–C) On top line diagrams are shown depicting the respective *HoxD* cluster configurations: wild-type (A), fully deleted (B) and partially deleted (C), with only *Hoxd11*, *Hoxd12* and *Hoxd13* left. The genotypes of the depicted limbs are indicated inscribed in the panels under the cluster diagrams. Below, palm clay prints of heterozygous *Gli3* mutants are shown, carrying two wild-type haplotypes of the *HoxD* cluster (D, *Xt/+;+/+*), one wild-type haplotype and one copy of the *del(1–13)* allele (E, *Xt/+;del(1–13)/+*) or one wild-type haplotype and one copy of the *Del(1–10)* allele (F, *Xt/+;Del(1–10)/+*). The pattern shown in panel D is not significantly different from wild-type and represents also the vast majority of *Del(1–10)* heterozygous (*+/+;Del(1–10)/+*) specimen. Digit pattern of *del(1–13)* heterozygous (*+/+; del(1–13)/+*) differs only marginally from wild-type, with slightly reduced digit 2 and digit 5 lengths (not shown). (G–L) Full forelimb skeletal preparations of late prenatal fetuses (E18) of the F2 generation derived from crosses of either *Xt/+;del(1–13)/+* (H, K) or *Xt/+; Del(1–10)/+* (G, J and I, L) parents are shown below. Humerus reductions in either the normal (I) or the *Gli3* deficient background (L) are much stronger in the presence of the *Hoxd11*, *Hoxd12* and *Hoxd13* genes; compare *+/+;Del(1–10)/Del(1–10)* and *Xt/Xt;Del(1–10)/Del(1–10)* with wild-type. Note also that the massive polydactyly that characterizes the *Gli3*-deficient background (J) remained in the absence of all *Hoxd* genes (K), whereas one to three digits form only in the presence of two doses of the *Del(1–10)* allele (L).

Skeletal preparations

Fetuses were collected by cesarean section on E18, photographed, tail biopsied, eviscerated and skinned for the Alizarin red and Alcian blue standard skeletal staining procedure (see e.g. www.eumorphia.org/EMPReSS/servlet/ EMPReSS Doc. Number: 12_005). Forelimb skeletons were dissected off, equilibrated into 80% glycerol, flat-mounted and photographed at identical magnification.

Results

Protective role of Gli3 against posterior prevalence

We crossed *Xt* mice (Figs. 1A, D) with mice either lacking the full *HoxD* cluster (Figs. 1B, E) or carrying a deletion from

Hoxd1 to *Hoxd10* (Figs. 1C, F) in order to assess whether the polydactyly induced by the null mutation of *Gli3* (*Xt/Xt;+/+*, Figs. 1G, J) is due to the de-repression, in time and space, of *Hox* gene function. Mice double homozygous for *Xt* and the *del(1–13)* allele (full deletion) were obtained and still displayed a severe polydactyly, as exemplified by forelimbs bearing seven to eight digital rods (Figs. 1H, K). This polydactyly was induced by the removal of *Gli3* function, as forelimbs of animals homozygous for the *del(1–13)* allele alone were mostly pentadactylous (Fig. 1H). In addition to the digit phenotype, forelimbs of double mutant animals were significantly and globally smaller than controls, the reduction including distal as well as proximal limb segments (Fig. 1K). This was unexpected as the absence of the entire *Hoxd* cluster (*del(1–13)/del(1–13)*)

produced only a minor reduction of the proximal limb (Fig. 1H). Furthermore, *Xt/Xt* mice also show such a reduction in the length of their hindlimbs (Barna et al., 2005; Chen et al., 2004).

A reduction in the length of the limbs was also scored in the second stock used in these crosses. We had previously reported that mice homozygous for the *Del(1–10)* allele displayed a double posterior digit pattern (Zakany et al., 2004), as a consequence of the establishment, at the anterior margin, of a second zone of *Shh* expression. This ectopic domain was triggered by the widespread expression of the remaining *Hoxd11*, *Hoxd12* and *Hoxd13* genes, likely under the transcriptional control of regulatory sequences located in 3′ of the cluster, which upon deletion would influence the expression of these genes (Tarchini and Duboule, 2006; Zakany et al., 2004). This gain of function phenotype showed some variability and a fair proportion of these limbs displayed both a reduced number of digits (oligodactyly) and a more or less severe limb shortening (Fig. 1I). Limb shortening was particularly evident in the stylopod (the humerus) and was substantially less pronounced in *del(1–13)* than in *Del(1–10)* mutant animals (Figs. 1H, I), supporting a gain of function effect as the causative factor. Altogether, these observations indicated that the abnormally early and proximal expression of *Hoxd11*, *Hoxd12* and *Hoxd13*, in *Del(1–10)* mice, impacted upon the growth potential of the limbs, in addition to the loss of function effect following the deletion of several *Hoxd* genes.

Surprisingly, animals carrying the partial deletion of the *HoxD* cluster *Del(1–10)*, associated with the absence of *Gli3*

function, almost completely lacked their forelimbs (Fig. 1L). This drastic phenotype was not scored with full deletions of the *HoxD* cluster (Fig. 1K), which suggested that a gain of function of the remaining *Hoxd* genes was likely involved. In such mice, the stylopod was completely lost and a single and truncated cartilage model, in the worst case, was observed at the position of the zeugopod. The autopods were just as severely reduced, displaying a single digit in the continuation of the zeugopod cartilage (Fig. 1L).

Because *Xt* homozygous mice, with or without a *HoxD* cluster, do not display such defects, we concluded that neither *Gli3* nor the *HoxD* cluster are strictly necessary for proximal limb development, even though their combined absence generated somewhat smaller limbs, suggesting a genetic interaction between *Gli3* and *HoxD* genes. In those mice where the absence of *Hoxd1* to *Hoxd10* was associated with ectopic expression of *Hoxd11*, *Hoxd12* and *Hoxd13* in the early limb bud (Zakany et al., 2004), subsequent growth was dramatically dependent on the presence of the *Gli3* product. This genetic analysis thus identified GLI3 as a factor protecting the developing limb from the deleterious effect of an early gain of function of 'posterior' *Hoxd* genes.

To document this interpretation, we looked at the level of both *Gli3* and *Hoxd13* transcripts in E9 limb buds of *Del(1–10)/Del (1–10)* mice. Indeed a number of *Del(1–10)/+* animals display hindlimb polydactyly (Zakany et al., 2004) and the majority of *Xt/+;Del(1–10)/+* mice (Fig. 1C) show anterior polydactyly, reminiscent of fetal *Xt/Xt* forelimbs, suggesting that *Gli3*
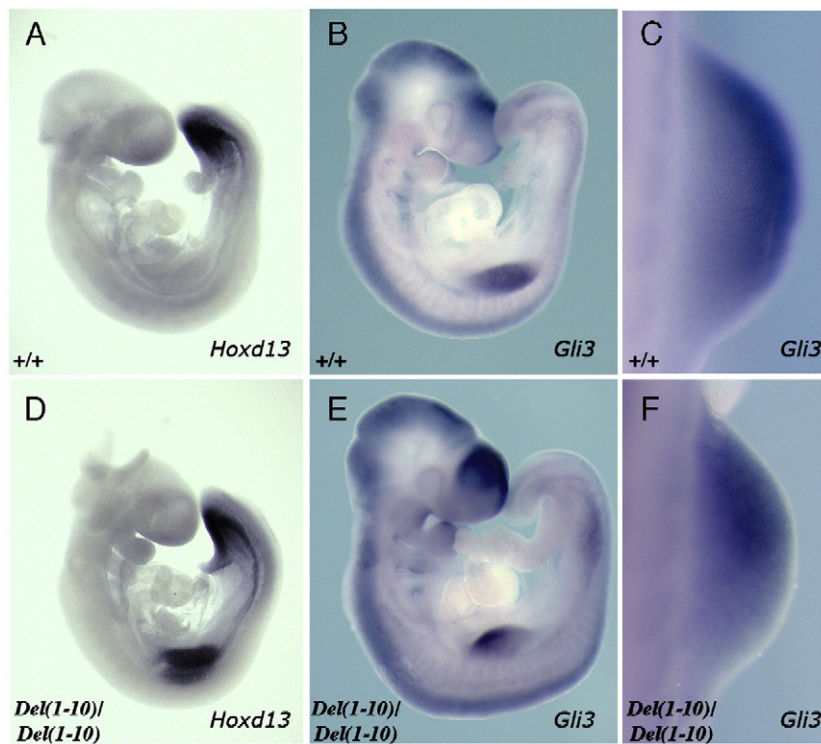

Fig. 2. Expression patterns of *Hoxd13* (A and D) and *Gli3* (B, C, E and F) in wild-type (A–C) and *Del(1–10)* homozygous (D–F) mid-gestation (E9) mouse embryos. All these specimen are wild-type at the *Gli3* locus. (A) *Hoxd13* expression is not yet detectable at this stage in wild-type, while the entire limb bud shows strong ectopic and premature *Hoxd13* transcript accumulation in *Del(1–10)* homozygous (D). Expression pattern of *Gli3* does not differ appreciably between wild-type and *Del(1–10)* homozygous (compare panels B to E and C to F).

expression may be modified in these stocks. The comparison between Figs. 2A and D demonstrates the ectopic and premature expression of *Hoxd13* in *Del(1–10)/Del(1–10)*, with a pattern including the entire incipient forelimb bud. At the same stage, *Gli3* transcript accumulation is comparable in these two genotypes (compare Figs. 2B, C and E, F), suggesting that the effect of ectopic posterior *Hoxd* gene expression is not mediated by a transcriptional suppression of *Gli3*. Furthermore, the co-expression of *Gli3* and posterior *Hoxd* genes in the limb bud mesenchyme make potential direct molecular interaction between these gene products possible.

Quantitative interactions

The GLI3-dependent suppression of *Hoxd13* and *Hoxd12* gain of function clearly depended upon the doses of both *Gli3* and the remaining *Hoxd* genes, as shown by the phenotypic distribution detailed in Fig. 3. Forelimbs either lacking only a single dose of *Gli3* (*Xt/+;+/+*) , or having a weak *Hoxd* gain of function in the presence of a full complement of *Gli3* (*+/+;Del(1–10)/+*) generally displayed a wild-type phenotype (Fig. 3; group II). Forelimbs lacking two doses of *Gli3* were polydactylous, but their humeri were of normal size (Fig. 3; I).

Reduction in the size of the stylopod started when trans-heterozygous animals were considered, i.e. those with only one dose of *Gli3* and one dose of gained *Hoxd11*, *Hoxd12* and *Hoxd13* (Fig. 3; III, IV). This latter reduction was close to that routinely seen in the homozygous *Del(1–10)* mutants, in the presence of two doses of *Gli3* (Fig. 3; IV).

Animals with three mutant alleles displayed slightly but significantly different phenotypic outcomes. In the presence of two doses of ectopic posterior *Hoxd* alleles combined with the loss of one dose of *Gli3*, the humerus was either severely reduced (7 out of 10; Fig. 3; V, VI) or virtually absent. The situation was similar when only one dose of ectopic posterior *Hoxd* alleles was combined with a complete absence of *Gli3*. This constitution also increased the severity of the phenotype (6 out of 10). Finally, animals lacking both doses of *Gli3* and harboring two doses of ectopic posterior *Hoxd* alleles had no trace of humerus, even though the remnants of both a zeugopod and an autopod were recognizable (Fig. 3; VI–VIII).

Effect upon the AER

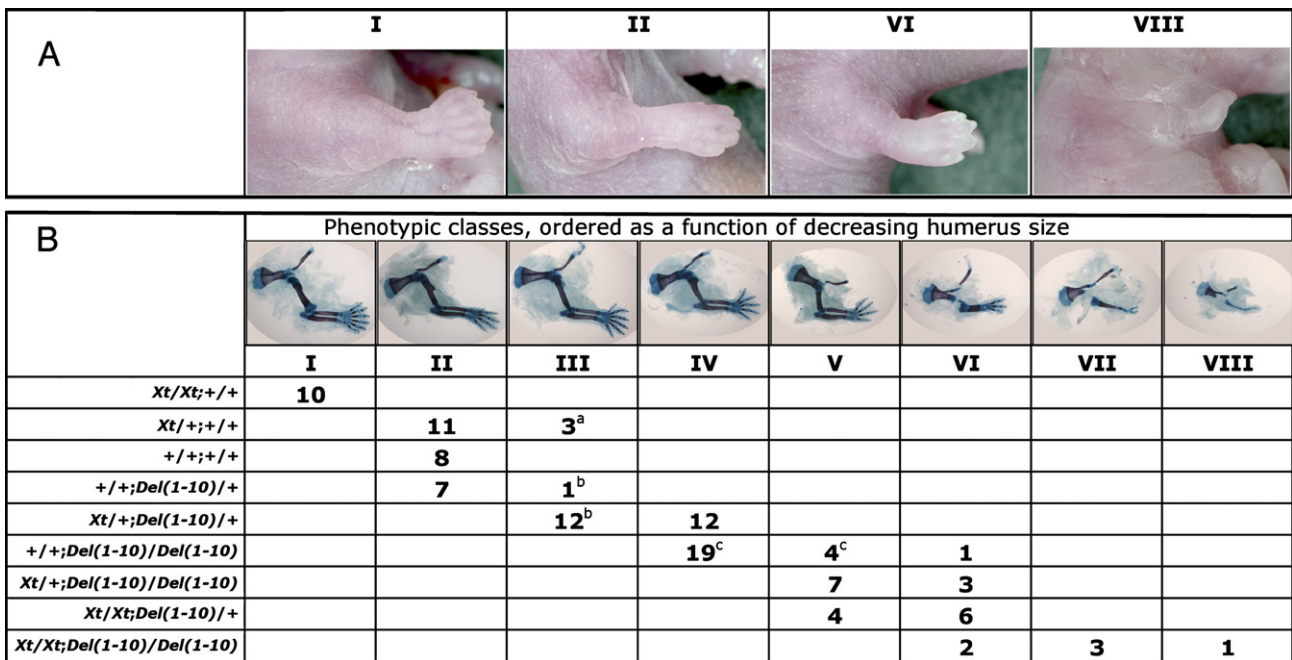The extent of skeletal truncations suggested that mutant limb development was compromised from a very early stage.

	I	II	III	IV	V	VI	VII	VIII
Xt/Xt;+/+	10							
Xt/+;+/+		11	3[a]					
+/+;+/+		8						
+/+;Del(1-10)/+		7	1[b]					
Xt/+;Del(1-10)/+			12[b]	12				
+/+;Del(1-10)/Del(1-10)				19[c]	4[c]	1		
Xt/+;Del(1-10)/Del(1-10)					7	3		
Xt/Xt;Del(1-10)/+					4	6		
Xt/Xt;Del(1-10)/Del(1-10)						2	3	1

Fig. 3. Variety of forelimb defects in *Xt, Del(1–10)* and compound mutant near-term mouse fetuses. (A) Gross morphology of *Xt* homozygous, wt, *Del(1–10)* homozygous and double homozygous forelimbs. *Xt* homozygous (*Xt/Xt;+/+*) forelimbs were easily recognized by the typical six or seven digit polydactyly. By contrast, the rest of the limb appeared relatively normal. A proportion of *Del(1–10)* homozygous (*+/+;Del(1–10)/Del(1–10)*) showed very short four- or three-digit oligodactylous limbs. All compound homozygous *Xt/Xt;Del(1–10)/Del(1–10)* displayed short oligodactylous limbs, including an extreme case of monodactyly. Roman numerals on the top (I, II, VI, VIII) indicate the phenotypic class allocations of the pictured newborns, as explained under (B). (B) Genotype distribution of skeletal patterns listed as eight phenotypic classes recovered in this stock. A representative picture is shown (I to VIII), and the classes are ordered from left to right according to decreasing limb proximal to distal length, reflecting the severity of the defect. In class I, both the humerus and overall limb size are normal, but with a polydactylous autopod. In classes II to V, a progressive reduction in the lengths of the humeri can be seen. In classes V to VIII, the humerus is completely absent. In class VI, the middle bony elements are identified as radius and ulna, although they are more tightly apposed to one-another. In classes VII and VIII, a single skeletal element is found between the strongly reduced scapula and digit(s). This element can hardly be identified with anything present in normal limbs. In class VIII, no ossification is apparent distal to the scapula. When the genotype of the *Gli3* locus is kept identical, increasing the dose of the *Del(1–10)* allele increased the severity of the phenotype. Likewise, when keeping the mutant genotype at the *HoxD* locus identical (either *Del(1–10)/+*, or *Del(1–10)/Del(1–10)*), increasing the dose of wild-type *Gli3* reduced the severity of the alterations.

Accordingly, we collected F2 embryos at E10 from *Xt/+;Del(1–10)/+* compound heterozygous parents. Genotyping and anatomical examination revealed that all possible genotypes were represented in near Mendelian proportions and that all mutant embryos showed the clear presence of limb buds. Therefore, initial limb budding occurs in compound mutants, indicating that size reductions mostly developed later, during and after E10, a stage corresponding to the establishment of the apical ectodermal ridge (AER).

Several genetic activities are necessary for the formation, maintenance and function of the AER, such as the mesenchymal factors *Fgf10* and *Shh*, or ectodermal factors like *Fgf8*. These genes are normally expressed at the time when ectopic *Hoxd11*, *Hoxd12* and *Hoxd13* expression is scored in the *Del(1–10)* allele, which also induces an ectopic *Shh* domain. We examined the expression of *Hoxd13*, *Fgf10*, *Shh* and *Fgf8* in the various

genotypic classes described in Fig. 3. Representative forelimb buds of four of these genotypic classes are documented in Fig. 4. Examples of the corresponding skeletal patterns at E18 are included for direct comparison.

In wild-type limb buds, *Hoxd13* and *Hoxd12* expression is first restricted to the most posterior part of the budding limb (early phase in Tarchini and Duboule, 2006). Soon after, expression of these genes *de novo* appears in the future digit domain, at the postero-distal part of the outgrowing bud, under a different transcriptional control (Tarchini and Duboule, 2006). Consequently, E10 limb buds show both this emergent domain (Fig. 4A; arrow), as well as more proximal weakly expressing cells, remnant of the early posterior domain seen at E9 (Fig. 4A; arrowhead). An important effect of this early and posterior expression domain is to trigger *Shh* expression, which will thus be confined to posterior cells (Fig. 4C; (Tarchini et al., 2006). At
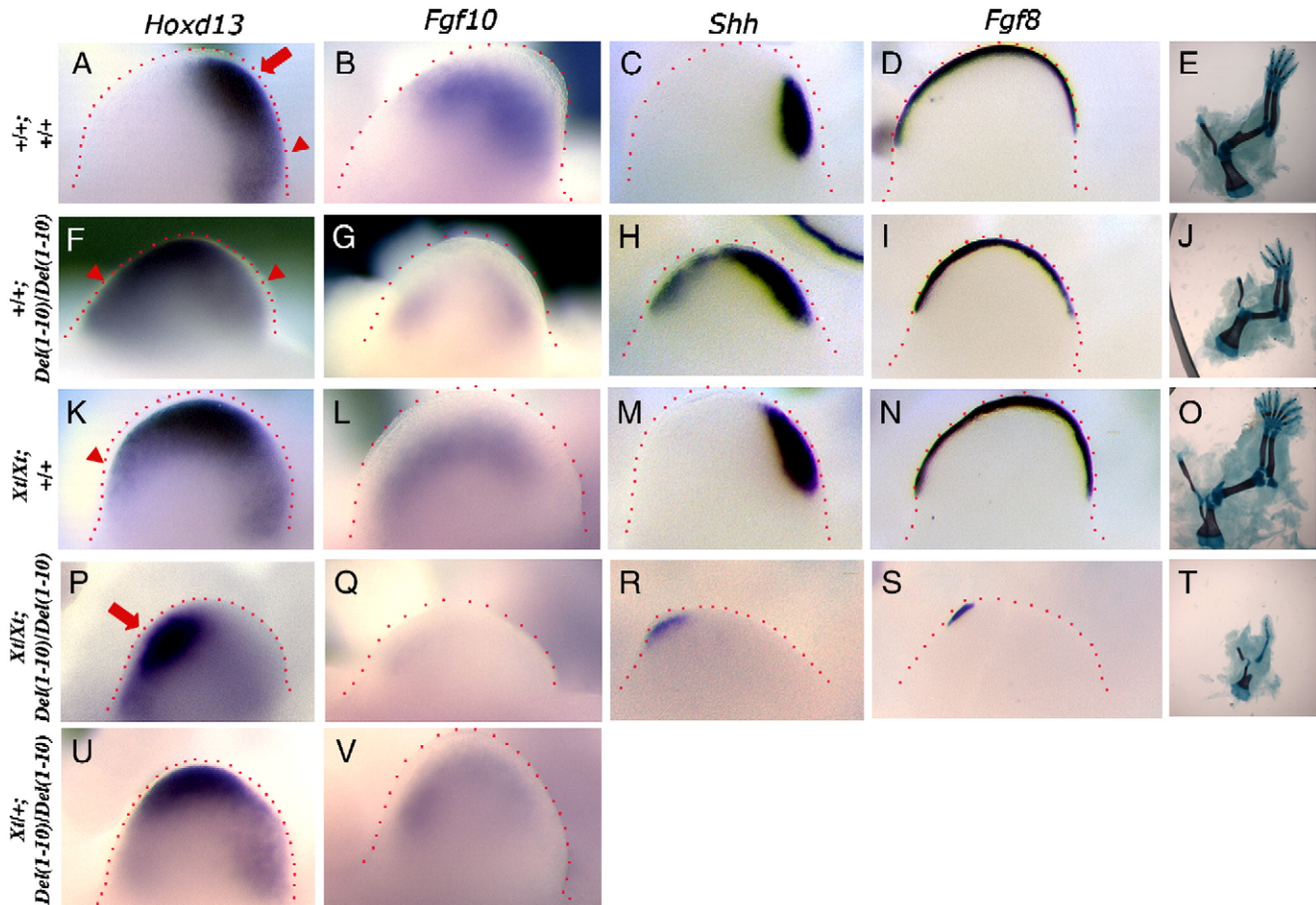

Fig. 4. Expression analyses of *Xt, Del(1–10)* and compound mutant forelimb buds. Whole mount *in situ* hybridization using *Hoxd13*, *Fgf10*, *Shh* and *Fgf8* probes were carried out on wild-type, *+/+;Del(1–10)/Del(1–10)*, *Xt/Xt;+/+*, *Xt/Xt;Del(1–10)/Del(1–10)* and *Xt/+;Del(1–10)/Del(1–10)* E10 embryos. Genotypes are indicated on the left, probes on the top. Panels in the right are representative skeletal E18 preparations to indicate the fate of those buds shown on the left panels. In *+/+; Del(1–10)/Del(1–10)* embryos, the expression patterns of *Hoxd13* (compare panels A and F), *Fgf10* (compare panels B and G) and *Shh* (compare panels C and H) were extended into more anterior regions, whereas *Fgf10* level was reduced and *Fgf8* seemed relatively normal (compare panels D and I). In *Xt/Xt;+/+Hoxd13* (K), *Fgf10* (L) and *Shh* (M), transcript profiles were extended into more anterior regions as well, whereas *Fgf10* level was somewhat reduced (compare panels B and L) and *Fgf8* seemed relatively normal, if not slightly increased (N). In *Xt/Xt;Del(1–10)/Del(1–10)* embryos, expressions of *Hoxd13* (P), *Fgf10* (Q) and *Shh* (R) were scored only in anterior regions. Interestingly both *Hoxd13*, *Fgf10* and *Shh* transcripts were hardly detectable in their normal domains and *Fgf8* was confined to a very tiny cluster of cells overlying the *Hoxd13*, *Fgf10* and *Shh*-positive domain (compare panels Q, R and S). Overall, limb buds from *+/+;Del(1–10)/Del(1–10)* and *Xt/Xt;Del(1–10)/ Del(1–10)* genotypes appeared smaller than wild-type, which was consistent with the subsequently observed reduction in the size of these limbs. As compared to *Xt/Xt; Del(1–10)/Del(1–10)* (P and Q) in *Xt/+;Del(1–10)/Del(1–10)* embryos the limb bud size (U and V) and *Fgf10* signal intensity (V) were significantly rescued by the presence of one wild-type copy of *Gli3* in presence of a well detectable ectopic *Hoxd13* signal throughout the anterior limb bud (U).

E10, *Fgf10* is expressed with a medial-posterior specificity, in a rather large domain. Positive cells nevertheless are excluded from the most distal parts of the bud (where *Hoxd13* appears stronger), as well as from most anterior cells (Fig. 4B). Throughout limb budding and early outgrowth, *Fgf8* expression extends along the anterior to posterior rim of the limb bud (Fig. 4D), indicating the presence of a well-established AER (Lewandoski et al., 2000).

Mutant limb buds showed clear deviations from these expression patterns. In *Del(1–10)* homozygous, general accumulation of *Hoxd13* transcripts in E9 buds (Zakany et al., 2004) leads to a visible anterior ectopic domain, mirroring wild-type posterior expressing cells (Fig. 4F; arrowheads). The late domain appeared in a more distal position, pre-figuring the bilateral symmetry of the limb. Following the de-localization of *Hoxd13* and *Hoxd12* expression domains, *Shh* appeared along the entire distal rim of the bud (Fig. 4H), to be subsequently split into two opposing domains, leading to the double-posterior morphology (Zakany et al., 2004). Expression of *Fgf10* in these mutant buds was clearly down-regulated, and scored both anteriorly and posteriorly, whereas mostly non-detected in the distal part where the late *Hoxd13* domain was visible (Fig. 4, compare F and G). Here again, expression matched the bilateral symmetry subsequently observed. Consistently, *Fgf8* expression did not substantially change, albeit the overall length of the AER was slightly reduced, consistent with the general reduction in the size of the limb bud (Fig. 4I).

Interestingly, *Xt/Xt* homozygous limb buds showed modifications of these expression patterns not drastically different from those observed in *Del(1–10)* deleted animals. *Hoxd13* early expression extended into the most anterior part of the bud (Zuniga and Zeller, 1999), and a remnant of this pattern was still detected at E10 (Fig. 4K, arrowhead), along with a rather distal domain for the late *Hoxd13* pattern. *Shh* expression was also somewhat extended along the anterior-distal margin (Fig. 4M), although much less extensively than *Hoxd13*, especially as anterior proximal, and also most part of the distal limb domains remained devoid of *Shh* transcripts until later, when an ectopic *Shh* domain is generally scored anteriorly (Buscher et al., 1997). *Fgf10* was slightly down-regulated but again extended into anterior distal and proximal domains (Fig. 4L). *Fgf8* expression was essentially identical to wild-type, indicating the presence of a near normal AER, corresponding to the seemingly normal aspect of these early limb buds, despite their subsequent polydactyly (Fig. 4N).

Xt/Xt;Del(1–10)/Del(1–10) compound animals displayed drastically different expression patterns. *Hoxd13* transcripts accumulated in the anterior limb bud, suggesting a complete shift in the anterior-posterior polarity of the bud. While this was observed for the late *Hoxd13* domain, traces of the early expression suggested a similar inversion of polarity (Fig. 4P; arrow). Accordingly, *Shh*-positive cells were found at an anterior-distal position, corresponding to cells expressing *Hoxd13* Fig. 4R). However, signal intensity was just above detection and only few cells were scored positive. *Shh* expression was not detected in its usual posterior domain. *Fgf10* expression was also severely reduced in quantity, and

mostly found in anterior mesenchymal cells, illustrating once again an inversion in the AP polarity (Fig. 4Q; see below). Finally, the pool of *Fgf8*-positive cells was also dramatically reduced. Only a small cluster of positive cells was detected in the anterior limb bud, precisely above the ectopic domains for all three *Hoxd13*, *Fgf10* and *Shh* (Fig. 4S). This virtually non-existing AER coincided with an important reduction in the size of the entire limb bud when compared to all other genotypes.

In *Xt/+;Del(1–10)/Del(1–10)* compound mutants, ectopic expression of *Hoxd13* in anterior regions was clearly detected as well, and a shift of the late distal domain towards the anterior margin was also evident, giving an overall pattern that was intermediate between *Xt/Xt;Del(1–10)/Del(1–10)* and *+/+;Del(1–10)/Del(1–10)*. Accordingly, the intensity of the *Fgf10* signal increased, and the size of the limb bud was also consistently bigger than that of the double homozygous. From this data set, we concluded that expressions of both *Fgf10* in the mesenchyme and *Fgf8* in the newly forming AER were severely altered in the presence of prematurely expressed *Hoxd13* and *Hoxd12*, provided the quantity of GLI3 was either reduced, or completely absent. Because both *Gli3* and *Hoxd* genes are expressed in mesenchyme, we favored an hypothesis whereby these latter gene products would act upon *Fgf10* transcript accumulation. In double mutants, *Fgf10* was massively affected, which prevented formation of a full-grown AER leading to the observed truncations.

Fgf10 in early mutant limb buds

We looked at the expression of *Fgf10* in earlier mutant limb buds, i.e. at a stage where the AER was being established, hence gene expression was unlikely to depend upon AER derived signals (Fig. 5). Two major aspects were immediately scored: firstly, the presence of two copies of the *Del(1–10)* mutant allele drastically reduced the quantity of *Fgf10* transcripts, regardless of the presence or absence of *Gli3* function (Figs. 5B, C). Secondly, the absence of *Gli3* function (*Xt/Xt*) induced a spectacular inversion of AP polarity, independently of the presence or absence of the *Del(1–10)* allele (Figs. 5C, D; see also Fig. 4). Concerning the former aspect, it is likely that the down-regulation of *Fgf10* depended upon the presence of gained posterior *Hox* genes, as two copies of the *Del(1–10)* allele were required to achieve substantial extinction of *Fgf10*, in the absence of *Gli3* function.

The inversion of *Fgf10* polarized expression was mostly dependent upon the absence of *Gli3* function, as it started to occur even with a normal set of *Hox* genes (Fig. 4). In this case, a 'rotation' of the *Fgf10* pattern was scored, along with the distalization of the *Shh* expressing domain (Fig. 4L, compare Fig. 4M). While *Del(1–10)* homozygous limb buds had a bilateral expression of *Fgf10*, following that of posterior *Hoxd* genes, further removing *Gli3* function gave the limb a clear, yet not sustainable, inverted polarity (Figs. 4 and 5). Up-regulation of *Fgf10* in the anterior bud may result from the observed gain of posterior *Hoxd11* gene expression there upon loss of *Gli3* function (Zuniga and Zeller, 1999). Likewise, *Del(1–10)* mutant limb buds may induce *Fgf10* expression anteriorly. The
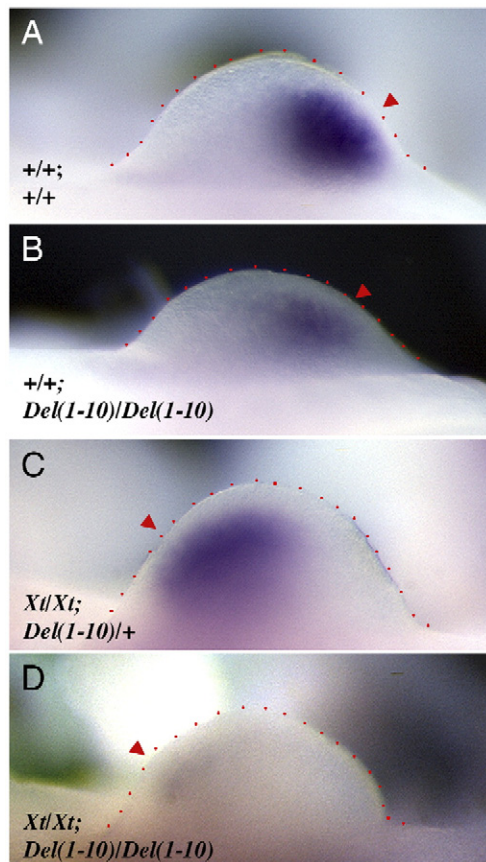
Fig. 5. Suppression of *Fgf10* transcript accumulation in pre-AER stage mutant limb buds and inversion of the anterior to posterior polarity. In normal limb buds (A), *Fgf10* accumulation occurred preferentially in the posterior part (indicated by red arrowhead on the right). (B) In homozygous *Del(1–10)* animals, *Fgf10* transcript accumulation was significantly reduced, yet still detected in the expected posterior domain. (C, D) When the two mutations were combined, an inversion of polarity in the distribution of *Fgf10* was observed (indicated by red arrowhead on the left). In compound homozygous very low level of *Fgf10* signal could be detected (D). When the *HoxD* gain of function was reduced by half, in *Xt/Xt;Del(1–10)/+* mutant (C), transcript accumulation in this anterior domain increased substantially. Therefore, both in the presence and in the absence of *Gli3*, premature posterior *Hoxd* gene expression suppressed *Fgf10* gene transcript level, though this suppression was increased by removing *Gli3* function, leading to more severe truncations (see Figs. 1 and 3).

disappearance of *Fgf10* expression from the posterior margin of the limb in *Del(1–10)/Xt* compound mutants may also reflect the down-regulation of posterior *Hoxd* genes in these cells, yet how the *Xt* mutation stimulates this remains elusive.

Discussion

Genetic analyzes have highlighted the role of the *HoxA* and *HoxD* clusters in tetrapod limb development (Davis et al., 1995; Kmita et al., 2005). Recently, their capacity to regulate the amount and position of *Shh* transcripts, hence to control both proximal to distal growth and the anterior to posterior polarity, was proposed (Tarchini et al., 2006). In this view, the late and posteriorly restricted expression of groups 10 to 13 *Hox* genes is mandatory for further development of the *Shh*-dependent, most distal part of the limb. However, combined *HoxA/HoxD* clusters

deficient limbs showed more extensive truncations than those reported for *Shh* mutant mice (Chiang et al., 2001; Kmita et al., 2005), suggesting that *Hox* gene products are required early on, independent of their effect upon *Shh* transcription, likely to control the formation or maintenance of the AER. In this work, we provide evidence that the integrity of the AER depends on the interplay between posterior *Hoxd* genes and *Gli3*, probably mediated through the control of *Fgf10* expression in early limb bud mesenchyme.

Antagonistic role of 5′ HOXD genes and GLI3 in controlling FGF10

When *Gli3* was either half, or fully abrogated, in the presence of prematurely expressed *Hoxd13* and *Hoxd12*, extreme limb truncations occurred. Interestingly, the most affected limbs, in this phenotypic series resembled those observed either after surgical removal of the AER in chick limb buds (Saunders, 1948) or after inactivation of *Fgf* signaling in mice. Genetic analyses of limb development in mice identified *Fgf10* as a major early mesenchymal competence factor (Sekine et al., 1999) and further studies on *Fgf* receptors have associated this early step with the establishment of the AER (Li et al., 2005; Revest et al., 2001; Xu et al., 1998), which will be subsequently the source of *Fgf4* and *Fgf8*. Inactivation of *Fgf8* impacted upon the formation of the stylopod (Lewandoski et al., 2000) and additional inactivation of *Fgf4* prevented the development of all three limb segments. Interestingly, in *Fgf8;Fgf4* compound mutants, *Fgf10* expression was severely reduced, whereas *Shh* transcription was abrogated (Boulet et al., 2004; Sun et al., 2002), pointing to feedback mechanisms in this complex process.

In our experiments, expression of *Fgf10* in the mesenchyme and of *Fgf8* in the forming AER were dramatically reduced, indicating a defect in the *Fgf10* to *Fgf8* arm of the positive circuit maintaining AER function. This important decrease in the amount of *Fgf10* transcripts resulted from prematurely expressed *Hoxd13* and *Hoxd12* genes. Yet this effect was not observed, or at least not to this degree, in the presence of the *Gli3* gene product. Therefore, *Gli3* products were able to mitigate, or protect from, the effects of *Hoxd* gain of function upon *Fgf10* activity, in a dose-dependent manner. In *Del1–10* homozygous mice, initial *Fgf10* expression was indeed readily detectable, whereas only trace amounts of *Fgf10* could still be seen after additional removal of *Gli3* function. In such double mutants, patches of AER were occasionally scored with only dispersed *Fgf8*-positive cells, suggesting that, receiving weak *Fgf10* signal, epidermal cells started responding by activating *Fgf8* transcription, but the pool of responding cells was likely too small and failed to assemble a ridge. In the development of the final phenotype, these most severe constitutions are tantamount to a genetic AER ablation. From previous experiments, in particular those involving simultaneous inactivation of *Fgf8* and *Fgf4,* it is expected that massive apoptosis is involved in bringing about the eventual truncations (Sun et al., 2002). Besides fibroblast growth factors, other signals are involved in AER establishment (Capellini et al., 2006; Hill et al.,

2006; Mariani and Martin, 2003) and we cannot rule out the possibility that other signaling cascades be directly affected by this HOX/GLI3 circuitry.

'Anterior' Hox genes promote AER formation

The deletion of both *HoxA* and *HoxD* clusters lead to severely compromised AER integrity and consequent arrest in the growth of limb buds (Kmita et al., 2005). Here, we show that a similar defect in the AER, associated with severe truncations, can be obtained even in the presence of the complete set of *Hoxa* genes, provided 'posterior' *Hoxd* genes are expressed ectopically and that *Gli3* function be removed. Collectively, these observations can be interpreted in the context of the 'posterior prevalence' rule (Duboule and Morata, 1994). In this view, 'anterior' *Hox* genes are required for proper AER establishment and/or function, whereas 'posterior' genes (e.g. groups 13 to 12) restrict AER longevity; the integration of differential *Hox* inputs being achieved by the regulation of *Fgf10* production. Accordingly, the correct balance, in time and space, between 'anterior' and 'posterior' *Hox* products may thus be central to proper proximal to distal outgrowth, by determining both the onset and the regression of the AER. The fact that transgene-driven expression of either *Hoxb8* (Charite et al., 1994) or *Hoxa9* (Williams et al., 2006) during early mouse limb development induced polydactyly and enlarged limb buds is compatible with an increase of AER output as a consequence of exaggerated 'anterior' *Hox* gene function.

In *Del(1–10)* homozygous animals, the gain of function of *Hoxd12* and *Hoxd13* in the anterior part of the early limb bud did not drastically impair AER formation. Instead, an ectopic *Shh* domain was observed anteriorly, leading to the formation of a bilateral symmetric limb, slightly reduced in length. When further removing the *Gli3* function, a drastic effect was seen on AER formation, which prevented the assessment of the effect upon *Shh* transcription, even though a weak domain was sometimes observed at a distal and anterior position. Therefore, we conclude that GLI3 does not interfere with the capacity of *Hoxd13*, *Hoxd12* or *Hoxd11* to trigger *Shh* expression. In contrast, *Gli3* products appear to protect anterior *Hoxd* gene products against the prevalent effect of posterior products and concurrent impairment of AER formation. While the underlying molecular mechanism is elusive, the fact that GLI3 and posterior HOX products directly bind to each other (Chen et al., 2004) suggest that GLI3 may sequester HOX products, thus preventing their deleterious effects. Whether or not this protective effect of GLI3 occurs in wild-type physiological conditions is more difficult to assess. The facility of obtaining proximal limb truncation upon ectopic expression of *Hoxd13* in transgenic mice, even in presence of a full complement of Gli3 (Williams et al., 2006) may reflect excessive amounts of ectopic products. Also, posterior HOX products must be expressed early enough to elicit *Shh* induction (from groups 10 to 13; Tarchini et al., 2006), at a time when the AER is being fully established. It is thus conceivable that GLI3 products would prevent this latter

structure to be aborted, in the case where these prevalent HOX proteins would be present.

Inversion of the AP polarity

In limb buds with both posterior *Hoxd* gene gain of function, and loss of *Gli3* function, a striking inversion of polarity was observed before the growth of the limb aborted due to the absence of AER. This inversion of polarity involves two separate changes: the gain of expression of several genes in the anterior part of the bud, and the concurrent loss of expression of the same genes in the posterior part. We believe this inversion follows posterior *Hoxd* gene ectopic expression, which is itself due the combined effect of the *Del(1–10)* gain of function (Zakany et al., 2004) and the absence of *Gli3*-mediated *Hox* repression in the anterior bud (Zuniga and Zeller, 1999). In the *Del(1–10)* deletion, *Hoxd11*, *Hoxd12* and *Hoxd13* are placed near the telomeric end of the cluster, where they fall under the control of regulatory elements that normally act on 'anterior' *Hox* genes. Therefore, these remaining three genes acquired a more anterior type of expression pattern in the early bud (Zakany et al., 2004), corresponding to the anterior specificity of those genes located in 3′ of the cluster (Tarchini et al., 2006). This anteriorization was nevertheless not complete, likely due to the property of *Gli3* to antagonize posterior *Hoxd* gene in the anterior limb bud, leading to the symmetrical distribution of e.g. *Hoxd13*.

However, whenever the dose of *Gli3* was reduced, a full anteriorization of the patterns was observed, as a result of the reduction in (or absence of) *Gli3*-mediated repression. The full anterior pattern of posterior *Hoxd* genes, as illustrated by *Hoxd13* (Fig. 4) was expectedly able to elicit *Shh* transcription in an anterior spot (Tarchini et al., 2006), underlying the few *Fgf8*-positive AER cells. A fully inverted limb was nonetheless impossible to produce since the protective effect of *Gli3* against posterior prevalence had been removed, leading to the concurrent growth arrest (see above).

Hox genes; a link between RA and Fgf signaling in limb buds?

The drastic defects observed in *Del(1–10);Xt* compound mutants limbs are remarkably similar to those described in animals with altered levels of retinoic acid, suggesting that related developmental pathways were affected in both cases. In the absence of endogenous RA synthesis, i.e. in animals lacking the function of *Raldh2*, the modifications in the expression of *Fgf10*, *Shh* and *Fgf8* were related to those reported in this paper. In particular, *Shh* was lost in the normal posterior limb bud of *Raldh2* mutants, whereas appearing delocalized in the distal region (Mic et al., 2004; Niederreither et al., 2002). Furthermore, as a consequence of RA depletion, posterior *Hoxd* genes became prematurely and ectopically expressed in early limb buds (Niederreither et al., 2002). These analogies suggest that an important role for RA signaling is to prevent posterior *Hox* genes to be transcribed in the early bud. In the absence of RA, *Hoxd12* and *Hoxd13* transcription was activated

prematurely and altered *Fgf10* gene expression, thus precluding bud growth.

On the other hand, in embryos mutated for the *Cyp261b* gene, i.e. with an increased level of RA, *Hoxd12* and *Hoxd13* transcription in limb buds was delayed (Yashiro et al., 2004) leading to severe defects in the stylopod, zeugopod and autopod. Interestingly, the eventual phenotypes of *Raldh2* and *Cyp261b* mutant limbs are quite alike, involving massive alterations of all limb regions, including the humerus. These phenotypes nevertheless arise through distinct mechanisms, as witnessed by the expression pattern of *Fgf8* in the AER: while reduced in *Raldh2* mutant, it was increased in *Cyp261b* mutants, in good correlation with either increased, or decreased *Hoxd12* and *Hoxd13* expression, respectively. The most severe genetic constitutions we report in this work are reminiscent to early vitamin A deficiencies. We tested the expression of *Meis1*, a gene that is under the control of RA signaling (Fig. S1) and observed normal expression patterns of this gene in our five key mutant combinations. We take this as an evidence that RA signal was initially received from the flank and that *Fgf*-dependent suppression of *Meis1* transcript accumulation in proximal bud was effective (Mercader et al., 2000).

The function of RA in the activation of *Hox* gene transcription has been abundantly documented, both on particular *Hox* genes, via their RAREs (Serpente et al., 2005) and at the level of entire clusters. In this latter case, RA was able to trigger collinear *Hox* genes activation in cultured EC cells (Simeone et al., 1990). It is thus possible that RA plays a role in the sequential activation of *Hox* genes during limb bud development by favoring expression of anterior *Hox* genes first, while delaying expression of the posterior members. This would allow for the AER to be established and functional, via *Fgf10* regulation, before the massive expression of posterior genes in the autopods would abrogate it. In this task of maintaining posterior *Hox* genes silent or harmless, RA would be helped by *Gli3*, first by its repressive effect on posterior *Hox* gene transcription in anterior cells (Zuniga and Zeller, 1999) then by the protective effect against potential posterior HOX products, which we describe in this work.

However, this explanatory framework fails to account for the fact that no major proximal defect occurs in *Gli3* minus animals, i.e. in the presence of detectable ectopic posterior *Hox* genes products in the early anterior limb bud (Zuniga and Zeller, 1999). We think that this may result from a dose effect, the amount and sustainability of these ectopic products being much below those observed in the *Del(1–10)* gain of function (Zakany et al., 2004). Also, in the *Gli3* mutant limb buds, ectopic posterior products must 'compete' against (or abrogate) the full complement of anterior *Hox* genes, whereas the complete set of anterior *Hoxd* genes is removed in the *Del(1–10)* mutants, in addition to a strong gain of expression. Such a dosage effect is well supported by the trans-heterozygous phenotypes described above. The fact that limbs develop well in the absence of *Gli3* function, despite the strong expression of posterior *Hoxd* genes in the distal autopod (late phase in Tarchini et al., 2006), suggests that the dramatic phenotypes observed in this work derive from perturbations occurring at a very early stage of limb bud development, a stage critical for the formation of the AER, in agreement with the described kinetics of the posterior *Hoxd* gene gain of function in *Del(1–10)* animals (Zakany et al., 2004).

Appendix A. Supplementary data

Supplementary data associated with this article can be found, in the online version, at doi:10.1016/j.ydbio.2007.03.517.

References

Barna, M., Pandolfi, P.P., Niswander, L., 2005. Gli3 and Plzf cooperate in proximal limb patterning at early stages of limb development. Nature 436, 277–281.

Bellusci, S., Grindley, J., Emoto, H., Itoh, N., Hogan, B.L., 1997. Fibroblast growth factor 10 (FGF10) and branching morphogenesis in the embryonic mouse lung. Development 124, 4867–4878.

Boulet, A.M., Moon, A.M., Arenkiel, B.R., Capecchi, M.R., 2004. The roles of Fgf4 and Fgf8 in limb bud initiation and outgrowth. Dev. Biol. 273, 361–372.

Buscher, D., Bosse, B., Heymer, J., Ruther, U., 1997. Evidence for genetic control of Sonic hedgehog by Gli3 in mouse limb development. Mech. Dev. 62, 175–182.

Capellini, T.D., Di Giacomo, G., Salsi, V., Brendolan, A., Ferretti, E., Srivastava, D., Zappavigna, V., Selleri, L., 2006. Pbx1/Pbx2 requirement for distal limb patterning is mediated by the hierarchical control of Hox gene spatial distribution and Shh expression. Development 133, 2263–2273.

Charite, J., de Graaff, W., Shen, S., Deschamps, J., 1994. Ectopic expression of Hoxb-8 causes duplication of the ZPA in the forelimb and homeotic transformation of axial structures. Cell 78, 589–601.

Chen, Y., Knezevic, V., Ervin, V., Hutson, R., Ward, Y., Mackem, S., 2004. Direct interaction with Hoxd proteins reverses Gli3-repressor function to promote digit formation downstream of Shh. Development 131, 2339–2347.

Chiang, C., Litingtung, Y., Harris, M.P., Simandl, B.K., Li, Y., Beachy, P.A., Fallon, J.F., 2001. Manifestation of the limb prepattern: limb development in the absence of sonic hedgehog function. Dev. Biol. 236, 421–435.

Crossley, P.H., Martin, G.R., 1995. The mouse Fgf8 gene encodes a family of polypeptides and is expressed in regions that direct outgrowth and patterning in the developing embryo. Development 121, 439–451.

Davis, A.P., Witte, D.P., Hsieh-Li, H.M., Potter, S.S., Capecchi, M.R., 1995. Absence of radius and ulna in mice lacking hoxa-11 and hoxd-11. Nature 375, 791–795.

Dolle, P., Dierich, A., LeMeur, M., Schimmang, T., Schuhbaur, B., Chambon, P., Duboule, D., 1993. Disruption of the Hoxd-13 gene induces localized heterochrony leading to mice with neotenic limbs. Cell 75, 431–441.

Duboule, D., 1991. Patterning in the vertebrate limb. Curr. Opin. Genet. Dev. 1, 211–216.

Duboule, D., Morata, G., 1994. Colinearity and functional hierarchy among genes of the homeotic complexes. Trends Genet. 10, 358–364.

Echelard, Y., Epstein, D.J., St-Jacques, B., Shen, L., Mohler, J., McMahon, J.A., McMahon, A.P., 1993. Sonic hedgehog, a member of a family of putative

signaling molecules, is implicated in the regulation of CNS polarity. Cell 75, 1417–1430.

Fromental-Ramain, C., Warot, X., Lakkaraju, S., Favier, B., Haack, H., Birling, C., Dierich, A., Dolle, P., Chambon, P., 1996a. Specific and redundant functions of the paralogous Hoxa-9 and Hoxd-9 genes in forelimb and axial skeleton patterning. Development 122, 461–472.

Fromental-Ramain, C., Warot, X., Messadecq, N., LeMeur, M., Dolle, P., Chambon, P., 1996b. Hoxa-13 and Hoxd-13 play a crucial role in the patterning of the limb autopod. Development 122, 2997–3011.

Goff, D.J., Tabin, C.J., 1997. Analysis of Hoxd-13 and Hoxd-11 misexpression in chick limb buds reveals that Hox genes affect both bone condensation and growth. Development 124, 627–636.

Herault, Y., Fraudeau, N., Zakany, J., Duboule, D., 1997. Ulnaless (Ul), a regulatory mutation inducing both loss-of-function and gain-of-function of posterior Hoxd genes. Development 124, 3493–3500.

Herault, Y., Rassoulzadegan, M., Cuzin, F., Duboule, D., 1998. Engineering chromosomes in mice through targeted meiotic recombination (TAMERE). Nat. Genet. 20, 381–384.

Hill, T.P., Taketo, M.M., Birchmeier, W., Hartmann, C., 2006. Multiple roles of mesenchymal beta-catenin during murine limb patterning. Development 133, 1219–1229.

Hui, C.C., Joyner, A.L., 1993. A mouse model of Greig cephalopolysyndactyly syndrome: the extra-toes mutation contains an intragenic deletion of the Gli3 gene. Nat. Genet. 3, 241–246.

Kmita, M., Duboule, D., 2003. Organizing axes in time and space; 25 years of colinear tinkering. Science 301, 331–333.

Kmita, M., Tarchini, B., Zakany, J., Logan, M., Tabin, C.J., Duboule, D., 2005. Early developmental arrest of mammalian limbs lacking HoxA/HoxD gene function. Nature 435, 1113–1116.

Kondo, T., Zakany, J., Innis, J.W., Duboule, D., 1997. Of fingers, toes and penises. Nature 390, 29.

Lewandoski, M., Sun, X., Martin, G.R., 2000. Fgf8 signalling from the AER is essential for normal limb development. Nat. Genet. 26, 460–463.

Li, C., Xu, X., Nelson, D.K., Williams, T., Kuehn, M.R., Deng, C.X., 2005. FGFR1 function at the earliest stages of mouse limb development plays an indispensable role in subsequent autopod morphogenesis. Development 132, 4755–4764.

Litingtung, Y., Dahn, R.D., Li, Y., Fallon, J.F., Chiang, C., 2002. Shh and Gli3 are dispensable for limb skeleton formation but regulate digit number and identity. Nature 418, 979–983.

Mariani, F.V., Martin, G.R., 2003. Deciphering skeletal patterning: clues from the limb. Nature 423, 319–325.

Mercader, N., Leonardo, E., Piedra, M.E., Martinez, A.C., Ros, M.A., Torres, M., 2000. Opposing RA and FGF signals control proximodistal vertebrate limb development through regulation of Meis genes. Development 127, 3961–3970.

Mic, F.A., Sirbu, I.O., Duester, G., 2004. Retinoic acid synthesis controlled by Raldh2 is required early for limb bud initiation and then later as a proximodistal signal during apical ectodermal ridge formation. J. Biol. Chem. 279, 26698–26706.

Niederreither, K., Vermot, J., Schuhbaur, B., Chambon, P., Dolle, P., 2002. Embryonic retinoic acid synthesis is required for forelimb growth and anteroposterior patterning in the mouse. Development 129, 3563–3574.

Revest, J.M., Spencer-Dene, B., Kerr, K., De Moerlooze, L., Rosewell, I., Dickson, C., 2001. Fibroblast growth factor receptor 2-IIIb acts upstream of Shh and Fgf4 and is required for limb bud maintenance but not for the induction of Fgf8, Fgf10, Msx1, or Bmp4. Dev. Biol. 231, 47–62.

Saleh, M., Huang, H., Green, N.C., Featherstone, M.S., 2000. A conformational change in PBX1A is necessary for its nuclear localization. Exp. Cell Res. 260, 105–115.

Saunders, J.W.J., 1948. The proximo-distal sequence of the origin of the parts of the chick wing and the role of the ectoderm. J. Exp. Zool. 108, 363–403.

Sekine, K., Ohuchi, H., Fujiwara, M., Yamasaki, M., Yoshizawa, T., Sato, T., Yagishita, N., Matsui, D., Koga, Y., Itoh, N., Kato, S., 1999. Fgf10 is essential for limb and lung formation. Nat. Genet. 21, 138–141.

Serpente, P., Tumpel, S., Ghyselinck, N.B., Niederreither, K., Wiedemann, L.M., Dolle, P., Chambon, P., Krumlauf, R., Gould, A.P., 2005. Direct cross-regulation between retinoic acid receptor {beta} and Hox genes during hindbrain segmentation. Development 132, 503–513.

Simeone, A., Acampora, D., Arcioni, L., Andrews, P.W., Boncinelli, E., Mavilio, F., 1990. Sequential activation of HOX2 homeobox genes by retinoic acid in human embryonal carcinoma cells. Nature 346, 763–766.

Spitz, F., Gonzalez, F., Duboule, D., 2003. A global control region defines a chromosomal regulatory landscape containing the HoxD cluster. Cell 113, 405–417.

Sun, X., Mariani, F.V., Martin, G.R., 2002. Functions of FGF signalling from the apical ectodermal ridge in limb development. Nature 418, 501–508.

Tarchini, B., Duboule, D., 2006. Control of Hoxd genes' collinearity during early limb development. Dev. Cell 10, 93–103.

Tarchini, B., Duboule, D., Kmita, M., 2006. Regulatory constraints in the evolution of the tetrapod limb anterior–posterior polarity. Nature 443, 985–988.

te Welscher, P., Zuniga, A., Kuijper, S., Drenth, T., Goedemans, H.J., Meijlink, F., Zeller, R., 2002. Progression of vertebrate limb development through SHH-mediated counteraction of GLI3. Science 298, 827–830.

van der Hoeven, F., Zakany, J., Duboule, D., 1996. Gene transpositions in the HoxD complex reveal a hierarchy of regulatory controls. Cell 85, 1025–1035.

Wang, B., Fallon, J.F., Beachy, P.A., 2000. Hedgehog-regulated processing of Gli3 produces an anterior/posterior repressor gradient in the developing vertebrate limb. Cell 100, 423–434.

Wellik, D.M., Capecchi, M.R., 2003. Hox10 and Hox11 genes are required to globally pattern the mammalian skeleton. Science 301, 363–367.

Williams, M.E., Lehoczky, J.A., Innis, J.W., 2006. A group 13 homeodomain is neither necessary nor sufficient for posterior prevalence in the mouse limb. Dev. Biol. 297, 493–507.

Xu, X., Weinstein, M., Li, C., Naski, M., Cohen, R.I., Ornitz, D.M., Leder, P., Deng, C., 1998. Fibroblast growth factor receptor 2 (FGFR2)-mediated reciprocal regulation loop between FGF8 and FGF10 is essential for limb induction. Development 125, 753–765.

Yashiro, K., Zhao, X., Uehara, M., Yamashita, K., Nishijima, M., Nishino, J., Saijoh, Y., Sakai, Y., Hamada, H., 2004. Regulation of retinoic acid distribution is required for proximodistal patterning and outgrowth of the developing mouse limb. Dev. Cell 6, 411–422.

Zakany, J., Kmita, M., Alarcon, P., de la Pompa, J.L., Duboule, D., 2001. Localized and transient transcription of Hox genes suggests a link between patterning and the segmentation clock. Cell 106, 207–217.

Zakany, J., Kmita, M., Duboule, D., 2004. A dual role for Hox genes in limb anterior–posterior asymmetry. Science 304, 1669–1672.

Zappavigna, V., Sartori, D., Mavilio, F., 1994. Specificity of HOX protein function depends on DNA-protein and protein-protein interactions, both mediated by the homeo domain. Genes Dev. 8, 732–744.

Zuniga, A., Zeller, R., 1999. Gli3 (Xt) and formin (ld) participate in the positioning of the polarising region and control of posterior limb-bud identity. Development 126, 13–21.